Spectrochimica Acta Part A 86 (2012) 276–288

Contents lists available at SciVerse ScienceDirect

Spectrochimica Acta Part A: Molecular and Biomolecular Spectroscopy

journal homepage: www.elsevier.com/locate/saa

Tetra- and hexadentate Schiff base ligands and their Ni(II), Cu(II) and Zn(II) complexes. Synthesis, spectral, magnetic and thermal studies

Tarek M.A. Ismail*, Akila A. Saleh, Mosad A. El Ghamry

Department of Chemistry, Faculty of Education, Ain Shams University, Roxy, Cairo, Egypt

ARTICLE INFO

Article history:
Received 6 June 2011
Received in revised form 10 October 2011
Accepted 14 October 2011

Keywords:
Schiff base derivatives
Schiff base complexes
Spectral
Magnetic
Thermal properties

ABSTRACT

Tetradentate N_2O_2, N_4 Schiff bases, 1,2-bis(4-oxopent-2-ylideneamino) benzene (BOAB), 1-(4-oxopent-2-ylideneamino-2-[(2-hydroxyphenyl)ethylideneamino] benzene (OAHAB), 7,16-bis(4-chlorobenzylidene)-6,8,15,17-tetra-methyl-7,16-dihydro -5,9,14,18-tetraza-dibenzo[a,h] cyclo tetradecene (BCBDCT), 7,16-bis(2-hydroxy-benzylidene)-6,8,15,17-tetramethyl-7,16-dihydro-5,9,14,18-tetraza-dibenzo [a,h] cyclo tetradecene (BHBDCT) and hexadentate N_4O_2 Schiff bases, 2,4-bis {2-[1-(2-hydroxyphenyl) ethylideneamino] phenylimino}-3-(2-hydroxybenzylidene) pentane (BHAPHP), 2,4-bis {2-[1-(2-hydroxyphenyl) ethylideneamino] phenylimino}-3-(4-chlorobenzylidene) pentane (BHAPCP) were prepared and characterized by elemental analysis, IR, UV–Vis, ^{1}H NMR and mass spectra. The solid complexes of the prepared Schiff base ligands with Ni(II), Cu(II) and Zn(II) ions were isolated and characterized by elemental and thermal analyses, IR, electronic and ESR spectra as well as conductance and magnetic susceptibility measurements. The results showed that most complexes have octahedral geometry but few can attain the tetrahedral arrangement. The TG analyses suggest high stability for most complexes followed by thermal decomposition in different steps. The kinetic and thermodynamic parameters for decomposition steps in Cu(II) complexes thermograms have been calculated.

1. Introduction

Metal complexes of Schiff bases occupy a central role in the development of coordination chemistry [1–6], the interest in the chemistry of Schiff base complexes lies in their importance in some biological processes such as the biological functions of bacteriorhodopsin [7], they can be used as biological models in understanding the structure of biomolecules [8–11] or metalloprotein models [12–14]. This is due to their resemblance to natural systems [15,16], also these compounds have received much attention as active parts of metalloenzymes [17,18]. Transition metal complexes of Schiff base compounds are used as growth inhibiting agents for most of bacteria and fungi [19–23] also they are widely used as potential therapeutics [24], they are useful in health and skin care [25]. The complexes of this type are also used as catalysis [26–33] for various chemical reactions. The Schiff base complexes of transition metal ions can be applied, particularly in the development of agrochemical and pharmaceutical industries [34].

In the present work, we have prepared new Schiff base compounds, (BOAB), (OAHAB), (BHAPHP), (BHAPCP), (BCBDCT) and (BHBDCT). The structures of these compounds were studied by elemental analysis, IR, UV–Vis, ^{1}H NMR and mass spectra. Then, their Ni(II), Cu(II) and Zn(II) complexes were prepared and the spectral, magnetic and thermal properties of these complexes were studied in detail. Also, the kinetic and thermodynamic parameters for decomposition steps in thermograms of Cu(II) complexes were calculated.

2. Experimental

2.1. Materials

Most of the chemicals used in the present investigation were BDH. Materials which are not generally provided into the analar grade were of highest available purity. They included *o*-phenylenediamine, acetylacetone, *p*-chlorobenzaldehyde, salicylaldehyde, *o*-hydroxyacetophenone, $NiCl_2 \cdot 6H_2O$, $CuSO_4 \cdot 5H_2O$ and $ZnSO_4 \cdot 7H_2O$. The solvents used were methanol, ethanol, dioxan and dimethylformamide (DMF), these solvents were either spectroscopically pure or purified by the recommended methods [35].

2.2. The apparatus and physical measurements

The elemental microanalyses of the prepared compounds for carbon, hydrogen, nitrogen, sulphur and chlorine were performed in the microanalytical center, Cairo University. The infrared spectra

---

* Corresponding author. Tel.: +20 1525659182.
E-mail address: tarek.ismail70@yahoo.com (T.M.A. Ismail).

1386-1425/$ – see front matter © 2011 Elsevier B.V. All rights reserved.
doi:10.1016/j.saa.2011.10.037

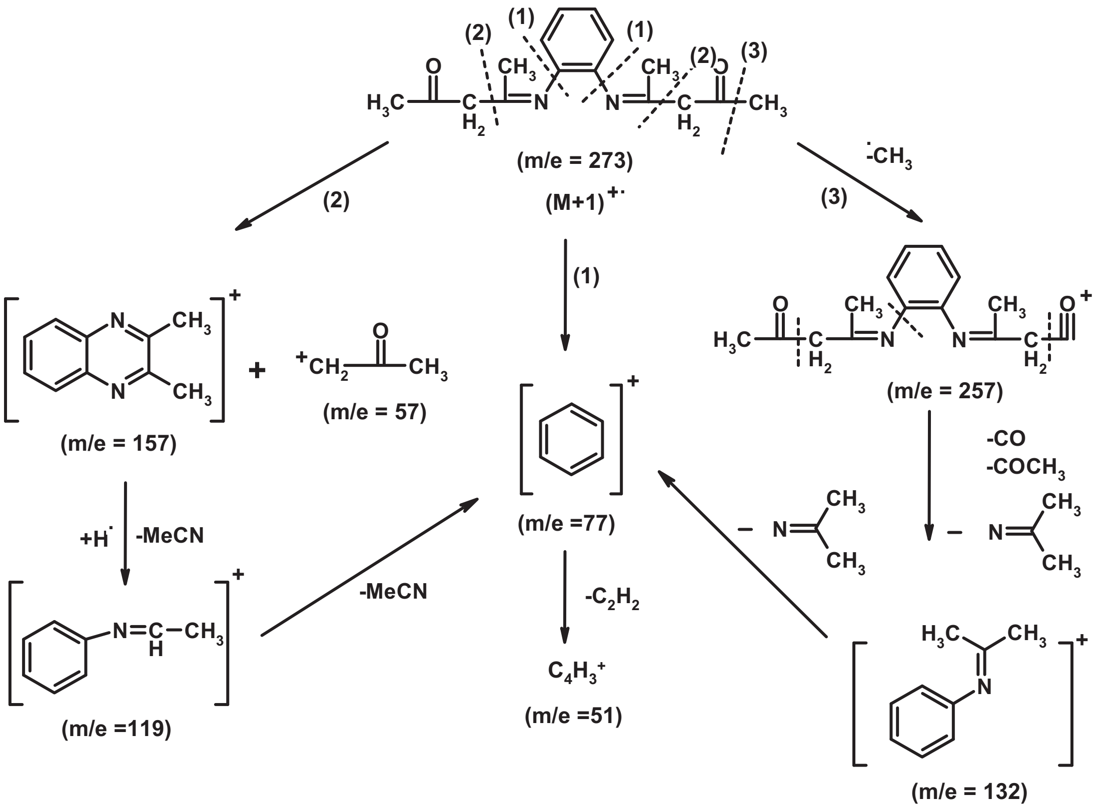

Scheme 1. Mass fragmentation pattern of (BOAB) compound.

were recorded using Bruker IR spectrometer in the microanalytical center of Azhar university within the range 4000–400 cm^{-1} and Perkin elmer 1430 IR spectrophotometer in the microanalytical center of Tanta university within the range 4000–200 cm^{-1}. IR spectra of the ligands and their solid complexes were obtained in the solid state using KBr disc technique. Nuclear magnetic resonance spectra were recorded by EM-3909, MHz NMR spectrometer, in the microanalytical center of Cairo University using d_6-DMSO, which was obtained from Alderich chemical company. The ultraviolet and visible spectra were recorded at room temperature over the wave length 200–850 nm by Jasco, V-550, UV–Vis. spectrophotometer using 1.0 cm matched silica cells. The molar conductance measurements were recorded using conductometer corning model 441. All measurements were performed at room temperature using DMF as solvent. The magnetic moment of the prepared metal complexes were determined at room temperature applying the Gouy's method using the magnetic susceptibility balance (CTM/Johnson Matthey Alfa products). Molecular susceptibilities were correct for diamagnetism of the component atoms applying the Pascal's constants [36]. Thermal analyses (TGA and DTA) of the solid complexes were performed at national drug research center using TGA-50 thermogravimetric analyzer (Shimadzu) from ambient temperature up to 800 °C with heating rate 10 °C/min using nitrogen atmosphere. Mass spectra were recorded by the aid of the Ms-5988 spectrometer, in the microanalytical center of Cairo university. The X-band ESR spectra of the powder complexes were recorded using Joel spectrometer model JES-FE2XG equipped with an E101 microwave bridge in the microanalytical center of Tanta University. The magnetic field was calibrated with 2,2-dipicryl hydrazyl. Metal contents of complexes were determined complexometrically using standard EDTA titration.

2.3. Preparation of the Schiff base compounds

2.3.1. Preparation of the compound (BOAB)

Acetylacetone (2.00 g, 0.02 mol) was added dropwise to *o*-phenylenediamine (1.08 g, 0.01 mol) in absolute ethanol (50 ml). The reaction mixture was refluxed on a hot plate for 6 h. The product was allowed to cool till room temperature, filtered off and recrystallized from ethanol then dried under vaccum to give dark brown crystals, yield 90%, m.p. 150 °C.

2.3.2. Preparation of 2-[(2-hydroxyphenyl) ethylideneamino]-phenylamine

A mixture of *o*-phenylenediamine (1.08 g, 0.01 mol) and *o*-hydroxyacetophenone (1.36 g, 0.01 mol) in absolute ethanol (50 ml) was refluxed for 8 h. The reaction mixture was concentrated to 20 ml then cooled to room temperature, filtered off, recrystallized from ethanol and dried under vaccum to give yellow crystals, yield 78%, m.p. 95 °C.

2.3.3. Preparation of the compound (OAHAB)

A mixture of 2-[(2-hydroxyphenyl)ethylideneamino]-phenylamine (2.26 g, 0.01 mol) and acetylacetone (1.00 g, 0.01 mol) in absolute ethanol (50 ml) was refluxed for 8 h. The reaction mixture was concentrated to 20 ml and then cooled to room temperature, filtered off, recrystallized from ethanol and dried under vacuum to give orange crystals, yield 85%, m.p. 192 °C.

2.3.4. Preparation of 2-hydroxy (or 4-chloro)-3-arylidene-2,4-pentanedione

A mixture of 2-hydroxybenzaldehyde (1.22 g, 0.01 mol) or 4-chlorobenzaldehyde (1.40 g, 0.01 mol) and acetylacetone (1.00 g, 0.01 mol) in absolute ethanol (50 ml) in the presence of two drops of piperidine was refluxed for 4 h. The reaction mixture was concentrated to 20 ml and then cooled to room temperature, filtered off, recrystallized from ethanol and dried under vaccum to give white or yellow crystals, m.p. 90 °C, 75 °C, yields 73% and 76%, respectively.

2.3.5. Preparation of the compounds (BHAPHP) and (BHAPCP)

A mixture of 2-[(2-hydroxyphenyl)ethylideneamino]-phenylamine (4.52 g, 0.02 mol) and 2-hydroxy-3-arylidene-2,4-pentanedione (2.04 g, 0.01 mol) or 4-chloro-3-arylidene-2,4-pentanedione (2.22 g, 0.01 mol) in absolute ethanol (50 ml) was refluxed for 8 h. The reaction mixture was concentrated to 20 ml and then cooled to room temperature, filtered off, recrystallized from ethanol and dried under vacuum to give brown crystals, m.p. 179 °C (BHAPHP) and 164 °C (BHAPCP), yields 75% and 78%, respectively.

2.3.6. Preparation of the compounds (BHBDCT) and (BCBDCT)

A mixture of *o*-phenylenediamine (2.16 g, 0.02 mol) and 2-hydroxy -3-arylidene-2,4-pentanedione (4.08 g, 0.02 mol) or 4-chloro-3-arylidene-2,4-pentanedione (4.45 g, 0.02 mol) in absolute ethanol (50 ml) was refluxed for 6 h. The reaction mixture was concentrated to 20 ml then cooled to room temperature, filtered off, recrystallized from ethanol and dried under vacuum to give brown crystals, m.p. 129 °C (BHBDCT) and 138 °C (BCBDCT), yields 79% and 82%, respectively.

The purity of the prepared Schiff base compounds was examined by elemental analysis, IR, ^{1}H NMR, UV–Vis and mass spectra. Anal. Calcd (BOAB): C, 70.59; H, 7.35; N, 10.29. Found: C, 70.19; H, 7.13; N, 9.92, Calcd (OAHAB): C, 74.03; H, 6.49; N, 9.09. Found: C, 73.51; H, 6.42; N, 8.61, Calcd (BHAPCP): C, 75.18; H, 5.48; N, 8.77; Cl, 5.56. Found: C, 74.91; H, 5.64; N, 8.61 Cl; 5.78, Calcd (BHAPHP)·2H_2O: C, 73.20; H, 6.10; N, 8.54. Found: C, 72.93; H, 5.91; N, 8.31, Calcd (BCBDCT): C, 73.34; H, 5.09; N, 9.51; Cl, 12.05. Found: C, 73.82; H, 5.05; N, 9.20; Cl, 11.95, Calcd (BHBDCT)·3/2 H_2O: C, 74.61; H, 6.05; N, 9.67. Found: C, 74.32; H, 6.11; N, 9.92. The color of the compound (OAHAB) was yellow while the another compounds were brown. IR (cm^{-1}), ν_{OH} of lattice H_2O molecules 3490–3528 for (BHAPHP) and (BHBDCT) compounds, ν_{OH} phenolic 3350–3462 for (OAHAB), (BHAPCP), (BHAPHP) and (BHBDCT) compounds, ν_{OH} enolic 3048–3070, $\nu_{C=O}$ 1704–1708, $\nu_{C=N}$ 1620–1640 for (BOAB) and (OAHAB) compounds, $\nu_{C=N}$ 1636–1645, 1590–1614 for (BHAPCP), (BHAPHP), (BCBDCT) and (BHBDCT) compounds. ^{1}H NMR, δ(ppm), δ_{OH} phenolic 9.60–12.30 for (OAHAB), (BHAPCP), (BHAPHP) and (BHBDCT) compounds, δ_{CH} aromatic 6.70–8.20, δ = CH 5.70–6.60, δ_{OH} enolic 5.20–5.60 for (BOAB) and (OAHAB) compounds, δ_{CH} aliphatic 2.00–2.60. The broad diffuse signals at 9.5–14.7 may be attributed to the presence of intramolecular hydrogen bonds between the phenolic OH or the enolic OH groups with the azomethine groups. UV–Vis spectra, λ_{max}(nm), the band located at (239–289) range is due to the low energy π–π^* transition of the aromatic system, C=C (L_b–L_A) [37], the band within the (312–408) range can be assigned to π–π^* transition within the C=N groups and the band within the (430–485) range is due to an intramolecular charge transfer within the whole molecule (CT). In case of (BOAB) and (OAHAB) compounds, there is another band within (273–342) range, due to π–π^* transition of C=O groups. The mass spectrum of the Schiff base (BOAB) as an example for the fragmentation of the Schiff bases under investigation is shown in Fig. 1, The fragmentation mode of (BOAB) [the molecular ion peak $(M+1)^{+\bullet}$ (m/e) = 273, I = 2.33)] occurs through three main pathways, Scheme 1. The Schiff base compounds have the following structural formulae:

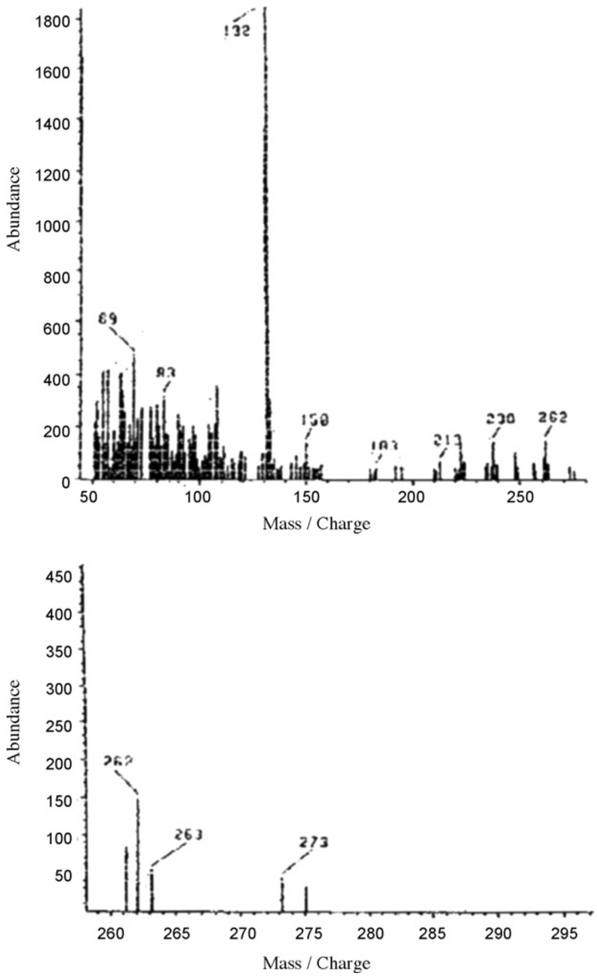

Fig. 1. Mass spectrum of (BOAB) compound.

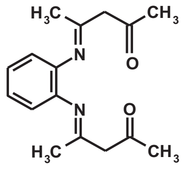

(BOAB)

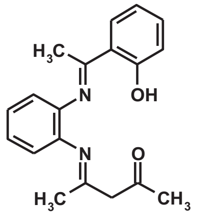

(OAHAB)

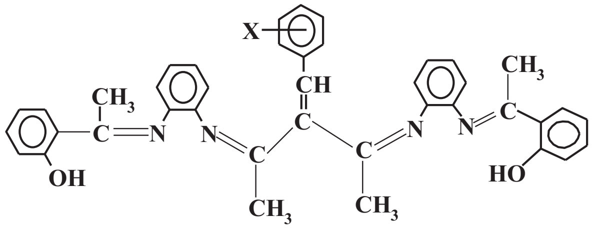

X = *p*-Cl (BHAPCP)
X = *o*-OH (BHAPHP)

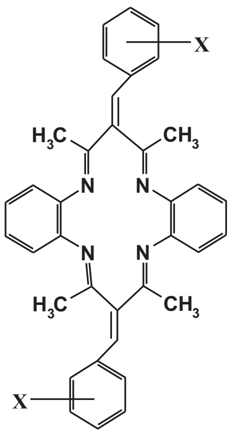

X = *p*-Cl (BCBDCT)
X = *o*-OH (BHBDCT)

2.4. Preparation of the solid complexes

The complexes ML were prepared by the reaction of Schiff base ligands with the metal sulphate or chloride in a (1:1) (L:M) molar ratio. 5 mmol of the metal salt, $NiCl_2.6H_2O$, $CuSO_4.5H_2O$ or $ZnSO_4.7H_2O$ dissolved in ethanol (10 cm^3) was added to 5 mmol of the ligand dissolved in ethanol (20 cm^3), the resulting solutions were stirred for about 1 hour, then refluxed on a hot plate from 6 to 8 hours. The solid complexes which separated out on hot were filtered off after cooling to room temperature, washed with small amounts of bidistilled water, ethanol and ether. The complexes were dried in vacuo, then subjected to elemental analysis, the results of microanalysis of the prepared complexes are collected in Tables 1 and 2.

3. Results and discussion

On the basis of elemental analysis, the transition metal ion complexes of Schiff base ligands were assigned to posses the compositions and molecular formulae listed in Tables 1 and 2. The results reveal that the ligands (BOAB), (OAHAB), (BCBDCT) and (BHBDCT) behave as neutral or dianionic tetradentate, while the ligands (BHAPCP) and (BHAPHP) behave as neutral or dianionic hexadentate towards the metal ions (Ni^{2+}, Cu^{2+} and Zn^{2+}).

The molar conductance of the metal complexes under investigation are measured for 10^{-3} M solution in DMF, Tables 1 and 2. Complexes (**1**, **3**, **4**, **5**, **9**, **10** and **13**) have Ω_m values in the range 8.0–13.0 ohm^{-1} cm^2 mol^{-1} which fall within the range of nonelectrolytes [38]. This indicates that $SO_4{}^{2-}$ and Cl^-ions are involved in the coordination sphere. Complexes (**11**), (**12**), (**14**), (**15**), (**16**) and (**17**) have Ω_m values in the range 72.6–87.1 ohm^{-1} cm^2 mol^{-1} which fall within the range of 1:1 electrolytes [38]. This indicates that $SO_4{}^{2-}$ and Cl^- ions are existing partially or completely in the outer sphere. The complexes (**2**, **6**, **7**, **8** and **18**) have Ω_m values in the range 136.2–147.0 ohm^{-1} cm^2 mol^{-1} which fall within the range of 1:2 electrolytes [38]. This indicates that $SO_4{}^{2-}$ and Cl^- ions are in the outer sphere.

3.1. Thermal analyses (TGA and DTA), kinetic and thermo-dynamic parameters studies of Cu(II) complexes

The results of thermal analyses (TGA and DTA) of Cu(II) complexes were recorded in Tables 3 and 4. The TGA curves of Cu(II) complexes show loss in weight within the temperature range 50–99 °C, which is due to removal of the lattice water molecules. Also, the Cu(II) complexes show mass loss within the temperature range 102–180 °C, which is due to removal of the coordinated

Table 1
Elemental analysis and some physical properties of the ligands (BOAB), (OAHAB), (BHAPCP) and their metal complexes.

	Complex	M:L	Color	M.P. (°C)	M. Wt. (gm)	Analysis (Calc. %) Found %						Ω_m (ohm^{-1} cm^2 mol^{-1})
						% C	% H	% N	% S	% Cl	% M	
(**1**)	$[Ni_2(BOAB)Cl_2]\cdot 2H_2O$	2:1	Brown	>300	494.4	(38.83) 38.52	(4.45) 5.05	(5.66) 6.04	–	(14.36) 13.71	(23.75) 23.35	11.44
(**2**)	$[Cu_2(BOAB)(H_2O)_6](SO_4)_2\cdot 2H_2O$	2:1	Dark brown	>300	735.0	(26.12) 26.11	(4.90) 4.11	(3.81) 2.81	(8.70) 8.36	–	(17.28) 16.88	141.20
(**3**)	$[Zn_2(BOAB)(SO_4)]\cdot 1/2H_2O$	2:1	Light brown	>300	505.6	(37.97) 38.22	(3.76) 3.73	(5.54) 5.91	(6.33) 7.30	–	(25.83) 25.76	13.0
(**4**)	$[Ni(OAHAB)(H_2O)_2]$	1:1	Pale green	>300	400.7	(56.90) 56.53	(5.49) 5.13	(6.99) 7.13	–	–	(14.65) 14.90	9.0
(**5**)	$[Cu(OAHAB)(H_2O)_2]$	1:1	Dark brown	>300	405.5	(56.22) 56.00	(5.42) 5.50	(6.90) 7.47	–	–	(15.67) 15.20	8.0
(**6**)	$[Zn_2(OAHAB)(H_2O)(EtOH)](SO_4)_2$	2:1	Reddish brown	>300	692.6	(36.38) 36.52	(3.75) 3.50	(4.04) 4.97	(9.24) 10.09	–	(18.86) 19.41	139.0
(**7**)	$[Ni(BHAPCP)]Cl_2$	1:1	Yellowish brown	>300	768.2	(62.48) 62.23	(4.56) 4.51	(7.29) 7.11	–	(13.86) 13.57	(7.64) 7.20	147.0
(**8**)	$[Cu_2(BHAPCP)(H_2O)_2](SO_4)_2$	2:1	Dark brown	>300	993.5	(48.31) 49.27	(3.93) 4.23	(5.64) 5.81	(6.44) 7.34	–	(12.78) 12.90	137.3
(**9**)	$[Zn_2((BHAPCP)(SO_4)]\cdot 4H_2O$	2:1	Reddish brown	>300	935.1	(51.33) 51.40	(4.38) 4.35	(5.99) 6.25	–	–	(13.97) 13.62	11.0

Table 2
Elemental analysis and some physical properties of the ligands (BHAPHP), (BCBDCT), (BHBDCT) and their metal complexes.

	Complex	M:L	Color	M.P. (°C)	M. Wt. (gm)	Analysis (Calc. %) Found %						Ω_m (ohm^{-1} cm^2 mol^{-1})
						% C	% H	% N	% S	% Cl	% M	
(**10**)	$[Ni_3(BHAPHP)(H_2O)_4Cl_3(OH)]\cdot 2H_2O$	3:1	Brown	>300	1025.6	(46.80) 46.04	(4.58) 4.21	(5.46) 6.14	–	(10.38) 10.22	(17.17) 16.90	11.1
(**11**)	$[Cu_2(BHAPHP)(H_2O)_6]SO_4\cdot 2H_2O$	2:1	Dark brown	>300	985.0	(48.73) 48.29	(5.08) 4.15	(5.69) 6.25	–	–	(12.89) 12.69	78.0
(**12**)	$[Zn_2((BHAPHP)(H_2O)_2]SO_4\cdot 2H_2O$	2:1	Pale brown	>300	916.6	(52.37) 51.83	(4.58) 4.49	(6.11) 6.11	–	–	(14.25) 13.92	72.6
(**13**)	$[Ni_2(BCBDCT)(H_2O)_2Cl_4]\cdot H_2O$	2:1	Brown	>300	902.4	(47.87) 47.19	(3.99) 4.27	(6.21) 6.24	–	(23.60) 23.80	(13.01) 12.80	11.0
(**14**)	$[Cu(BCBDCT)(H_2O)_2]SO_4\cdot 2H_2O$	1:1	Black	>300	820.54	(52.65) 51.97	(4.63) 4.13	(6.82) 7.27	–	–	(7.74) 8.20	78.4
(**15**)	$[Zn(BCBDCT)]SO_4\cdot 5H_2O$	1:1	Brown	>300	840.3	(51.41) 50.96	(4.76) 4.77	(6.66) 7.88	–	–	(7.77) 7.34	86.8
(**16**)	$[Ni(BHBDCT)Cl(H_2O)]Cl$	1:1	Yellowish green	210	699.6	(61.75) 61.30	(4.86) 5.83	(8.00) 8.99	–	(10.15) 10.19	(8.39) 8.10	87.1
(**17**)	$[Cu(BHBDCT)]SO_4$	1:1	Dark brown	>300	711.54	(60.71) 60.83	(4.50) 5.33	(7.87) 7.51	–	–	(8.93) 8.50	74.9
(**18**)	$[Zn_2(BHBDCT)(H_2O)_2](SO_4)_2\cdot H_2O$	2:1	Yellowish brown	180	928.6	(46.52) 46.44	(4.09) 4.80	(6.03) 6.27	(6.89) 7.27	–	(14.06) 13.81	136.2

Table 3
Results of thermal analyses (TGA) and (DTA) of Cu(II) complexes of the ligands (BOAB), (OAHAB) and (BHAPCP).

Complex	Formula and structure of compound (M.wt)	Temperature range (°C)	DTA peaks (°C)	% loss in weight Found (Calc.)	Decomposed product lost
(**2**)	$[Cu_2(BOAB)(H_2O)_6](SO_4)_2\cdot 2H_2O$ (735)	50–99	72 (exo)	5.46 (4.90)	Loss of two lattic H_2O molecules
		104–150	140.17 (exo)	3.86 (4.90)	Loss of two coordinated H_2O molecules
		155–180	170 (exo)	9.84 (9.80)	Loss of four coordinated H_2O molecules
		185–360		Thermal stability	The anhydrous complex is thermostable up to 360 °C
		365–420	392(exo)	25.61 (26.12)	Loss of two H_2SO_4 molecules
		425–705	590 (exo)	20.15 (19.32)	Loss of $C_8H_{14}O_2$
		710–800	738 (exo)	14.03 (14.15)	Loss of $C_6H_4N_2$
				21.05 (20.81)	Residue, $[Cu_2(O)_2(CO)_2]$
(**5**)	$[Cu(OAHAB)(H_2O)_2]$ (405.5)	110–160	65.56 (exo)	8.75 (8.88)	Loss of two coordinated H_2O molecules
		165–210		Thermal stability	The anhydrous complex is thermostable up to 210 °C
		215–570	456.97 (exo)	41.61 (42.66)	Loss of $C_{11}H_{11}NO$
		575–720		Thermal stability	
		725–800	776 (endo)	9.35 (10.11)	Loss of CH_3CONH_2 molecule
				40.29 (38.35)	Residue, $[Cu(C_2O_4H)_2(C_2O_4H_2)]$
(**8**)	$[Cu_2(BHAPCP)(H_2O)_2](SO_4)_2$ (993.5)	105–140	62.61 (exo)	4.67 (3.62)	Loss of two coordinated H_2O molecules
		145–205		Thermal stability	The anhydrous complex is thermostable up to 205 °C
		210–395	311.39 (exo)	19.51 (19.33)	Loss of two H_2SO_4 molecules
		400–800	553.46 (exo)	18.42 (19.17)	Loss of $C_{12}H_{11}Cl$
				57.40 (57.88)	Residue, $[Cu_2(OH)_2(C_{14}H_{13}N_2O)_2]$

Table 4
Results of thermal analyses (TGA) and (DTA) of Cu(II) complexes of the ligands (BHAPHP), (BCBDCT) and (BHBDCT).

Complex	Formula and structure of compound (M. Wt.)	Temperature range (°C)	DTA peaks (°C)	% loss in weight found (Calc.)	Decomposed product lost
(**11**)	$[Cu_2(BHAPHP)(H_2O)_6]SO_4{\cdot}2H_2O$ (985)	50–80	79.8 (endo)	4.20 (3.65)	Loss of two lattic H_2O molecules
		115–175	169.72 (exo)	11.46 (10.96)	Loss of six coordinated H_2O molecules
		180–250		Thermal stability	The anhydrous complex is thermostable up to 250 °C
		255–360	345 (exo)	9.77 (9.75)	Loss of one H_2SO_4 molecule
		365–530	520 (endo)	40.00 (40.10)	Loss of $C_{26}H_{23}O_2N_2$
		535–620		Thermal stability	
		625–800	700 (endo)	15.28 (16.14)	Loss of $C_{10}H_{11}N_2$
				19.29 (19.39)	Residue, $2[Cu(C_2O_4)]$
(**14**)	$[Cu(BCBDCT)(H_2O)_2]SO_4{\cdot}2H_2O$ (820.5)	50–80	75 (endo)	4.00 (4.39)	Loss of two lattic H_2O molecules
		102–140	120 (exo)	4.10 (4.39)	Loss of two coordinated H_2O molecules
		145–195		Thermal stability	The anhydrous complex is thermostable up to 195 °C
		200–280	215 (exo)	11.56 (11.70)	Loss of one H_2SO_4 molecule
		285–320		Thermal stability	
		325–520	400 (exo)	32.85(34.19)	Loss of $C_{18}H_{15}NCl$
		525–800	716 (exo)	29.48 (28.34)	Loss of $C_{12}H_{11}N_3Cl$
				18.01 (16.51)	Residue, $[Cu(C_2O_4H)_2(C_2O_4H_2)]$
(**17**)	$[Cu(BHBDCT)]SO_4$ (711.5)	190–240	212 (exo)	14.00 (13.49)	Loss of H_2SO_4 molecule
		245–300		Thermal stability	$[Cu(BHBDCT)(OH)_2]$ is thermostable up to 300 °C
		305–470	416 (exo)	50.56 (50.32)	Loss of $C_{24}H_{24}O_2N$
		475–800	625 (endo)	23.07 (23.89)	Loss of $C_{10}H_8N_3$
				12.37 (12.30)	Residue, $[Cu(C_2O_4)]$

water molecules. The dehydrated complexes (**2**), (**5**), (**8**), (**11**) and (**14**) are thermally stable up to 360 °C, 210 °C, 205 °C, 250 °C and 195 °C, respectively, then the Cu(II) complexes show mass loss within the temperature range 190–425 °C, which is due to removal of the SO_4^{2-} ions. Finally the complexes undergo decomposition of the organic ligands within the temperature range up to 800 °C, leading to the formation of the final products $[Cu_2(O)_2(CO)_2]$, $[Cu(C_2O_4H)_2(C_2O_4H_2)]$, $[Cu_2(OH)_2(C_{14}H_{13}N_2O)_2]$, $[Cu(C_2O_4)]$, $[Cu(C_2O_4H)_2\ (C_2O_4H_2)]$ and $[Cu(C_2O_4)]$ for complexes (**2**), (**5**), (**8**), (**11**), (**14**) and (**17**), respectively.

The DTA curves of the Cu(II) complexes show endothermic or exothermic peaks in the temperature range 50–99 °C which are due to removal of the lattic water molecules from the outer sphere, also Cu(II) complexes show exothermic peaks in the temperature range 102–180 °C which are due to removal of the coordinated water molecules from the inner sphere. The DTA curves of Cu(II) complexes also exhibit exothermic peaks within the temperature range 190–425 °C which are due to removal of the SO_4^{2-} ions existing outside the coordination sphere, after that the exothermic or endothermic peaks within the temperature range up to 800 °C may be due to lattice rearrangement, phase transformation or decomposition of the organic ligands leading to the formation of the final products [39].

The order, n and activation energy, E^* of the decomposition steps for Cu(II) complexes were determined from TGA results using the Coats–Redfern equation [40]:

$$\ln\left[\frac{\{1-(1-\alpha)^{1-n}\}}{(1-n)T^2}\right] = \left(\frac{M}{T}\right) + B \quad \text{for } n \neq 1 \tag{1}$$

$$\ln\left[\frac{\{-\ln(1-\alpha)\}}{T^2}\right] = \left(\frac{M}{T}\right) + B \quad \text{for } n = 1 \tag{2}$$

where $M = -E^*/R$ and $B = \ln(AR/\Phi E^*)$; E^*, R, A and Φ are the activation energy, gas constant, pre-exponential factor and heating rate, respectively, $n = 0, 0.33, 0.5, 0.66, 1$.

The other thermo kinetic parameters (ΔH^*, ΔS^*, ΔG^*) were calculated using the relationships:

$$\Delta H^* = E^* - RT$$

$$\Delta S^* = R\left[\ln\left(\frac{Ah}{KT}\right) - 1\right]$$

$$\Delta G^* = \Delta H^* - T\Delta S^*$$

where K is the Boltzmann constant and h is Plank′s constant. The order (n) and thermo kinetic parameters of the decomposition steps for the chosen complexes are listed in Table 5. From the obtained data, the following remarks can be pointed out:

1. The ΔS^* values for complexes were found to be negative. This indicates that the activated complex is more ordered than the reactants and/or the reactions are slow [41].
2. The values of ΔG^* increase significantly for the subsequently decomposition stages due to increasing the values of $T\Delta S^*$ from one step to another which override the values of ΔH^*. This increase reflects that the rate of removal of the subsequent ligand will be lower than that of the precedent ligand [42]. This may be attributed to the structural rigidity of the remaining complex after the explusion of one and more ligands, as compared with the precedent complex, which requires more energy for its rearrangement before undergoing any compositional change.
3. The positive values of ΔH^* means that the decomposition processes are endothermic.

Table 5
The order (n), temperature of decomposition and activation parameters (E^*, ΔH^*, ΔS^* and ΔG^*) for decomposition of the Cu(II) complexes.

Complex	Step	Order (n)	T (K)	E^* (KJ mol^{-1})	ΔH^* (KJ mol^{-1})	ΔS^* (KJ mol^{-1} K^{-1})	ΔG^* (KJ mol^{-1})
(**2**)	1st	0.66	72.0	3.138	2.540	−0.1703	14.802
	2nd	0.00	160.2	3.921	2.590	−0.1799	31.410
	3rd	0.33	228.0	4.494	2.599	−0.1779	43.160
	4th	0.66	532.5	7.667	3.242	−0.1744	96.110
	5th	0.33	590.0	7.669	2.766	−0.1802	109.084
	6th	0.00	738.0	8.722	2.589	−0.1817	136.684
(**5**)	1st	0.00	65.6	3.003	2.729	−0.1810	14.603
	2nd	0.66	457.0	7.947	4.149	−0.1794	86.135
	3rd	0.00	776.0	9.153	2.704	−0.1810	143.160
(**8**)	1st	0.66	62.6	2.972	2.452	−0.1697	13.075
	2nd	0.00	311.4	5.328	2.740	−0.1842	60.100
	3rd	0.00	553.5	8.296	3.696	−0.1875	107.477
(**11**)	1st	0.00	79.8	3.121	2.458	−0.1813	16.926
	2nd	0.00	169.7	4.012	2.602	−0.1799	33.131
	3rd	0.50	345.0	5.519	2.652	−0.1756	63.234
	4th	0.33	520.0	7.335	3.014	−0.1818	97.55
	5th	0.66	700.0	8.573	2.756	−0.1721	123.226
(**14**)	1st	0.50	75.0	3.100	2.477	−0.1737	15.505
	2nd	0.66	120.0	3.549	2.552	−0.1704	23.000
	3rd	0.00	191.0	4.416	2.829	−0.1821	37.610
	4th	0.33	400.0	6.076	2.752	−0.1805	74.952
	5th	0.33	716.0	9.132	3.182	−0.1820	133.494
(**17**)	1st	0.00	102.0	3.721	2.873	−0.1826	21.498
	2nd	0.66	416.0	6.454	2.997	−0.1750	75.797
	3rd	0.66	625.0	7.889	2.695	−0.1726	110.570

3.2. *Spectral measurements*

The main bands of IR spectra of the metal complexes and their tentative assignments are listed in Tables 6 and 7. All solid complexes (except complexes **7** and **17**) exhibit broad bands around 3330–3480 cm^{-1} which are attributed to ($_{\text{OH}}$ of water and/or EtOH molecules associated with the complexes. The disappearance of ($_{\text{OH}}$ enolic and/or ($_{\text{OH}}$ phenolic bands from the IR spectra of all complexes (except **2**, **6**, **7** and **8**), support the proton displacement from the OH groups through the metal ions. In case of complexes **2**, **6**, **7** and **8**, ($_{\text{OH}}$ enolic and/or ($_{\text{OH}}$ phenolic bands are shifted to lower wavenumbers by 33–90 and 30–130 cm^{-1}, respectively, which indicates the participation of OH groups in coordination to the metal ions through the lone pair of electrons on the oxygen [43]. This is confirmed by the existence of new bands at 510–592 cm^{-1}, which could be assigned to ($_{\text{M–O}}$ bands. The ($_{\text{C=N}}$ bands are shifted to lower wavenumbers by 12–48 and 10–35 cm^{-1}, indicating the coordination of the imino nitrogen atoms to the metal ions. This can be supported by the existence of new bands at 452–496 cm^{-1} which could be assigned to ($_{\text{M–N}}$ bands [44]. Complexes **1**, **10** and **13** show new bands at 325–348 cm^{-1} which can be assigned to ($_{\text{M–Cl}}$. The appearance of tow bands at 312,310 and 290,295 for complexes 10 and 13 suggest that tow of Cl ions are involved in bridging coordination [43]. The binuclear complexes **1**, **3** and **6** show new bands at 600–680 cm^{-1}, which can be assigned to μ-oxo, M–O–M [45–49]. The Cu(II) complex (**2**) shows a new weak band at 890 cm^{-1}, which can be assigned to 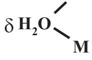 out of plane deformation of a water molecule acting as bridge between two metal ions [50]. For the complexes **2**, **6**, **8**, **11**, **12**, **14**, **15**, **17** and **18**, the ($_{\text{S–O}}$ are situated at 1106–1160, 970–1110 and 606–640 cm^{-1} which supports the non coordinated nature of the SO_4^{2-} ions [44]. For complexes **3** and **9**, IR spectra show splitted ($_{\text{S–O}}$ bands at 1164–1166, 1110–1112 and 1016–1018 cm^{-1} indicating the coordinated nature of SO_4^{2-} around the central metal ions [51,52].

The electronic absorption spectra of the metal complexes under investigation were recorded within the range 12,500–25,000 cm^{-1} applying the nujol mull technique and in DMF solution. The data obtained from these spectra are recorded in Table 8. The electronic spectra of Ni(II) complexes (**4**), (**7**), (**10**), (**13**) and (**16**) exhibit two bands with no obvious difference on going from nujol mull to DMF solution at (13,793–14,084, 15,015–15,384), cm^{-1}. These bands are assigned to $^3A_2g \rightarrow {}^3T_1g$ (F) and $^3A_2g \rightarrow {}^3T_1g$ (P) transitions which may indicate octahedral geometry around Ni(II) ions [53–55]. The electronic spectrum of Ni(II) complex (**1**) displays band at 13,698 cm^{-1} in DMF solution and at 14,706 cm^{-1} in nujol mull which can be assigned to $^3T_1 \rightarrow {}^3T_1$(P) transition indicating tetrahedral geometry around Ni(II) ion. The electronic spectra of Cu(II) complexes (**8**) and (**17**) in nujol mull show bands at 15,384 and 15,151 cm^{-1}, respectively, which can be assigned to $^2T_2g \rightarrow {}^2Eg$ transition within a tetrahedral structure. The positions of the bands of Cu(II) complexes in nujol mull spectra exhibit some shifts to lower wavelength in DMF solution to 16,129 and 15,873 cm^{-1}, respectively, indicating the facile formation of six coordinate species in DMF which is a coordinating solvent and tetrahedral geometry in the solid state. In case of Cu(II) complexes (**2**), (**5**), (**11**) and (**14**) the electronic spectra in DMF solution exhibit bands at (13,986–14,124, 15,974–16,207) cm^{-1} and in nujol mull at (13,888–14,084, 16,207–16,528) cm^{-1}, which can be assigned to $^2B_1g \rightarrow {}^2Eg$ and $^2B_1g \rightarrow {}^2B_2g$ transitions within octahedral structures [56].

3.3. *Magnetic properties of the metal complexes*

The effective magnetic moments of the prepared metal complexes were determined, the data obtained are listed in Table 8. The observed magnetic moment values of Ni(II) complexes were found to be in the range 2.50–2.74 B.M. These values indicate the presence of two unpaired electrons in the d-orbital, therefore, the complexes formed have either tetrahedral geometry as in complex (**1**) or an octahedral geometry as in complexes (**4**), (**7**), (**10**), (**13**) and (**16**). The values show the presence of some spin–spin interaction

Table 6

Important IR spectral data (cm^{-1}) and their assignment for ligands (BOAB), (OAHAB), (BHAPCP) and their metal complexes.

	Compound or complex	$^{\nu}H_2O$ and/or EtOH	ν_{OH} phenolic	ν_{OH} enolic	$\nu_{C=O}$	$\nu_{C=N}$	$\nu_{(M-O-M)}$	ν_{M-O}	ν_{M-N}	ν_{M-Cl} $\nu_{Cl-M-Cl}$	Other bands
	(BOAB)	–	–	3048	1708	1640	–	–	–	–	–
(**1**)	$[Ni_2(BOAB)Cl_2]\cdot 2H_2O$	3348	–	–	–	1594	680	548	485	348	–
(**2**)	$[Cu_2(BOAB)(H_2O)_6](SO_4)_2\cdot 2H_2O$	3480	–	3015	–	1612	–	552	488	–	ν_{S-O} 1108, 970, 616
(**3**)	$[Zn_2(BOAB)(SO_4)]\cdot 1/2H_2O$	3444	–	–	–	1592	652	592	452	–	$^{\nu}SO_4^{2-}$ 1166, 1112, 1018
	(OAHAB)	–	3350	3070	1704	1620	–	–	–	–	–
(**4**)	$[Ni(OAHAB)(H_2O)_2]$	3430	–	–	–	1596	–	544	496	–	–
(**5**)	$[Cu(OAHAB)(H_2O)_2]$	3404	–	–	–	1595	–	550	470	–	–
(**6**)	$[Zn_2(OAHAB)(H_2O)(EtOH)](SO_4)_2$	3420	3320	2980	–	1580	600	545	490	–	ν_{S-O} 1148,1110, 616
	(BHAPCP)	–	3456	–	–	1645, 1610	–	–	–	–	–
(**7**)	$[Ni(BHAPCP)]Cl_2$	–	3408	–	–	1624, 1590	–	530	472	–	–
(**8**)	$[Cu_2(BHAPCP)(H_2O)_2](SO_4)_2$	3435	3326	–	–	1618, 1575	–	540	490	–	ν_{S-O} 1140, 1104, 628
(**9**)	$[Zn_2((BHAPCP)(SO_4)]\cdot 4H_2O$	3440	–	–	–	1630, 1590	–	525	452	–	$^{\nu}SO_4^{2-}$ 1164, 1110, 1016

Table 7

Important IR spectral data (cm^{-1}) and their assignment for ligands (BHAPHP), (BCBDCT), (BHBDCT) and their metal complexes.

	Compound or complex	$^{\nu}H_2O$ and/or EtOH	ν_{OH} phenolic	$\nu_{C=N}$	ν_{M-O}	ν_{M-N}	ν_{M-Cl} $\nu_{Cl-M-Cl}$	Other bands
	$(BHAPHP)\cdot 2H_2O$	3528	3462	1638, 1590	–	–	–	–
(**10**)	$[Ni_3(BHAPHP)(H_2O)_4Cl_3(OH)]\cdot 2H_2O$	3398	–	622, 1580	520	472	325 310, 290	–
(**11**)	$[Cu_2(BHAPHP)(H_2O)_6]SO_4\cdot 2H_2O$	3450	–	1626, 1580	510	475	–	ν_{S-O} 1160,1108, 640
(**12**)	$[Zn_2((BHAPHP)(H_2O)_2]SO_4\cdot 2H_2O$	3330	–	1616, 1570	560	490	–	ν_{S-O} 1140,1102, 628
	(BCBDCT)	–	–	1636	530	472	–	–
(**13**)	$[Ni_2(BCBDCT)(H_2O)_2Cl_4]\cdot H_2O$	3438	–	1610	–	485	331 312, 295	–
(**14**)	$[Cu(BCBDCT)(H_2O)_2]SO_4\cdot 2H_2O$	3470	–	1592	–	460	–	ν_{S-O} 1112, 1016, 616
(**15**)	$[Zn(BCBDCT)]SO_4\cdot 5H_2O$	3444	–	1595	–	476	–	ν_{S-O} 1106, 1030, 606
	$(BHBDCT)\cdot 3/2H_2O$	3490	3363	1614	–	–	–	–
(**16**)	$[Ni(BHBDCT)Cl(H_2O)]Cl$	3350	–	1598	530	474	–	–
(**17**)	$[Cu(BHBDCT)]SO_4$	–	–	1590	540	452	–	ν_{S-O} 1110,1014, 620
(**18**)	$[Zn_2(BHBDCT)(H_2O)_2](SO_4)_2\cdot H_2O$	3430	–	1592	520	485	–	ν_{S-O} 1112,1016, 614

Table 8
Electronic absorption spectral data (cm^{-1}) and magnetic moment values of Ni(II) and Cu(II) complexes in nujol mull and DMF solution.

	Complex formula	Bands assignment due to d–d transition ν^{-} (cm^{-1})										$\mu_{eff.}$ (B.M.)
		Nujol mull				DMF						
		ν^{-} (cm^{-1})	d–d transition	ν^{-} (cm^{-1})	d–d transition	ν^{-} (cm^{-1})	ε (mol^{-1} cm^{-1} L)	d–d transition	ν^{-} (cm^{-1})	ε (mol^{-1} cm^{-1} L)	d–d transition	
(**1**)	$[Ni_2(BOAB)Cl_2]\cdot 2H_2O$	14,706	$^3T_1 \rightarrow {}^3T_1$ (P)	–	–	13,698	390	$^3T_1 \rightarrow {}^3T_1$ (P)	–	–	–	2.65
(**4**)	$[Ni(OAHAB)(H_2O)_2]$	13,815	$^3A_2g \rightarrow {}^3T_1g$ (F)	14,905	$^3A_2g \rightarrow {}^3T_1g$ (P)	13,793	125	$^3A_2g \rightarrow {}^3T_1g$ (F)	15,015	100	$^3A_2g \rightarrow {}^3T_1g$ (P)	2.50
(**7**)	$[Ni(BHAPCP)]Cl_2$	13,995	$^3A_2g \rightarrow {}^3T_1g$ (F)	15,300	$^3A_2g \rightarrow {}^3T_1g$ (P)	13,986	325	$^3A_2g \rightarrow {}^3T_1g$ (F)	15,384	250	$^3A_2g \rightarrow {}^3T_1g$ (P)	2.74
(**10**)	$[Ni_3(BHAPHP)(H_2O)_4Cl_3(OH)]\cdot 2H_2O$	14,084	$^3A_2g \rightarrow {}^3T_1g$ (F)	15,105	$^3A_2g \rightarrow {}^3T_1g$ (P)	14,035	280	$^3A_2g \rightarrow {}^3T_1g$ (F)	15,151	190	$^3A_2g \rightarrow {}^3T_1g$ (P)	2.68
(**13**)	$[Ni_2(BCBDCT)(H_2O)_2Cl_4]\cdot H_2O$	13,850	$^3A_2g \rightarrow {}^3T_1g$ (F)	15,082	$^3A_2g \rightarrow {}^3T_1g$ (P)	13,875	230	$^3A_2g \rightarrow {}^3T_1g$ (F)	15,135	180	$^3A_2g \rightarrow {}^3T_1g$ (P)	2.64
(**16**)	$[Ni(BHBDCT)Cl(H_2O)]Cl$	13,927	$^3A_2g \rightarrow {}^3T_1g$ (F)	15,243	$^3A_2g \rightarrow {}^3T_1g$ (P)	13,954	240	$^3A_2g \rightarrow {}^3T_1g$ (F)	15,222	170	$^3A_2g \rightarrow {}^3T_1g$ (P)	2.70
(**2**)	$[Cu_2(BOAB)(H_2O)_6](SO_4)_2\cdot 2H_2O$	13,888	$^2B_1g \rightarrow {}^2Eg$	16,207	$^2B_1g \rightarrow {}^2B_2g$	13,986	180	$^2B_1g \rightarrow {}^2Eg$	15,974	230	$^2B_1g \rightarrow {}^2B_2g$	1.52
(**5**)	$[Cu(OAHAB)(H_2O)_2]$	13,947	$^2B_1g \rightarrow {}^2Eg$	16,339	$^2B_1g \rightarrow {}^2B_2g$	14,044	110	$^2B_1g \rightarrow {}^2Eg$	16,077	185	$^2B_1g \rightarrow {}^2B_2g$	1.63
(**8**)	$[Cu_2(BHAPCP)(H_2O)_2](SO_4)_2$	15,384	$^2T_2g \rightarrow {}^2Eg$	–	–	16,129	360	$^2T_2g \rightarrow {}^2Eg$	–	–	–	1.55
(**11**)	$[Cu_2(BHAPHP)(H_2O)_6]SO_4\cdot 2H_2O$	14,005	$^2B_1g \rightarrow {}^2Eg$	16,447	$^2B_1g \rightarrow {}^2B_2g$	14,084	300	$^2B_1g \rightarrow {}^2Eg$	16,181	520	$^2B_1g \rightarrow {}^2B_2g$	1.57
(**14**)	$[Cu(BCBDCT)(H_2O)_2]SO_4\cdot 2H_2O$	14,084	$^2B_1g \rightarrow {}^2Eg$	16,528	$^2B_1g \rightarrow {}^2B_2g$	14,124	175	$^2B_1g \rightarrow {}^2Eg$	16,207	190	$^2B_1g \rightarrow {}^2B_2g$	1.67
(**17**)	$[Cu(BHBDCT)]SO_4$	15,151	$^2T_2g \rightarrow {}^2Eg$	–	–	15,873	250	$^2T_2g \rightarrow {}^2Eg$	–	–	–	1.65

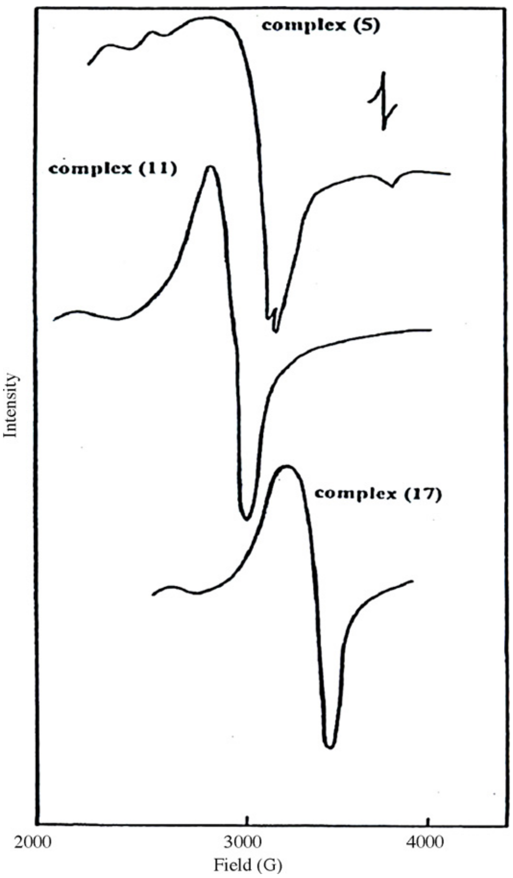

Fig. 2. ESR spectra of Cu(II) complexes (**5**), (**11**) and (**17**).

between the Ni(II) ions in the different complexes. The observed magnetic moment values of Cu(II) complexes were found to be in the range 1.52–1.67 B.M. this means that only one unpaired electron is present in the d-orbital [57]. Therefore, these complexes have either tetrahedral geometry as in complexes (**8**) and (**17**) or octahedral geometry as in complexes (**2**), (**5**), (**11**) and (**14**). For complexes (**2**), (**8**) and (**11**) the results indicate some spin-spin coupling due to antiferromagnetic interaction [58].

3.4. ESR spectra of Cu(II) complexes

ESR spectra of Cu(II) complexes have been recorded at room temperature as shown in Fig. 2. The g_{eff} values are calculated and recorded in Table 9. The shape of ESR signals and the g_{eff} values which are 2.45, 2.65, 2.65 and 2.64 for Cu(II) complexes (**2**), (**5**), (**11**) and (**14**), respectively, indicate octahedral geometries around Cu(II) ions in these complexes, where three anisotropic signals are observed. While in case of complexes (**8**) and (**17**) only two lines are observed, the shape of signals and the g_{eff} value which are 1.87 and 1.89, respectively, may indicate tetrahedral geometries around Cu(II) ions in these complexes. From the observed g-values of the Cu(II) complexes, it is clear that $g_{II} > g_{\perp}$ which indicates that the unpaired electron is predominantly in the dx^2–y^2 orbital [59–61] giving ^2B_1g as the ground state. The observed data show that the g_{II} values are >2.0023 for complexes (**2**), (**5**), (**11**) and (**14**) and hence the metal–ligand bonding in these complexes are essentially covalent, while for complexes (**8**) and (**17**) the g_{II} values are <2.0023, hence the metal–ligand bonding in the complexes are of appreciable ionic character [62].

Table 9
ESR data of Cu(II) complexes.

Complex no.	Complex formula	$g_{\parallel}$	$g_{\perp}$	$g_{eff.}$	Geometry
(**2**)	$[Cu_2(BOAB)(H_2O)_6](SO_4)_2{\cdot}2H_2O$	2.13	2.68	2.45	Octahedral
(**5**)	$[Cu(OAHAB)(H_2O)_2]$	2.72	2.58	2.65	Octahedral
(**8**)	$[Cu_2(BHAPCP)(H_2O)_2](SO_4)_2$	1.90	1.83	1.87	Tetrahedral
(**11**)	$[Cu_2(BHAPHP)(H_2O)_6]SO_4{\cdot}2H_2O$	2.85	2.44	2.65	Octahedral
(**14**)	$[Cu(BCBDCT)(H_2O)_2]SO_4{\cdot}2H_2O$	2.81	2.46	2.64	Octahedral
(**17**)	$[Cu(BHBDCT)]SO_4$	1.90	1.87	1.89	Tetrahedral

4. Conclusion

Based on the above results gained from elemental analyses, conductance measurements, thermal analyses, IR, UV–Vis, ESR spectra as well as magnetic moments studies, the geometric structures of the complexes under investigation can be formulated as follows:

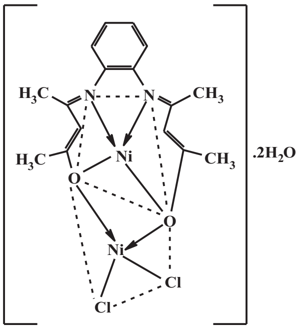

(1)

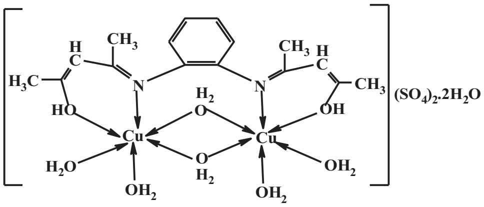

(2)

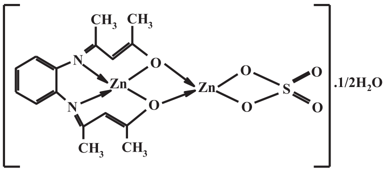
CH₃
CH₃
N
Zn
O
Zn
O
S
O
N
O
CH₃
CH₃
.1/2H₂O

(3)

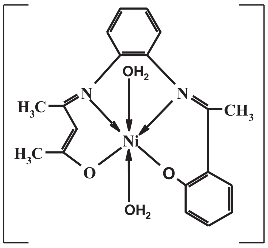
OH₂
N
N
H₃C
CH₃
Ni
H₃C
O
O
OH₂

(4)

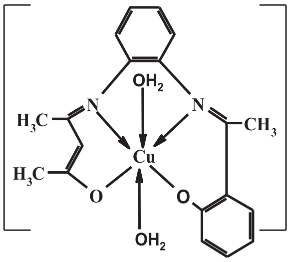
OH₂
N
N
H₃C
CH₃
Cu
H₃C
O
O
OH₂

(5)

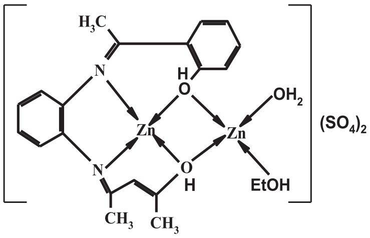
H₃C
N
H
O
OH₂
Zn
Zn
(SO₄)₂
N
O
H
EtOH
CH₃
CH₃

(6)

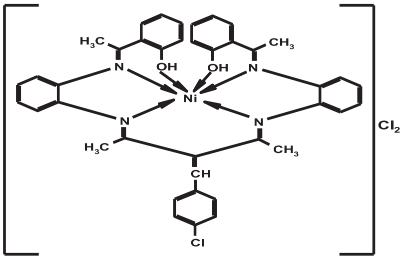
H₃C
CH₃
N
OH
OH
N
Ni
N
N
Cl₂
H₃C
CH₃
CH
Cl

(7)

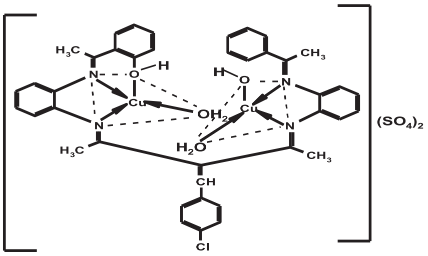
H₃C
CH₃
N
O
H
H
O
N
Cu
OH₂
Cu
(SO₄)₂
N
H₂O
N
H₃C
CH₃
CH
Cl

(8)

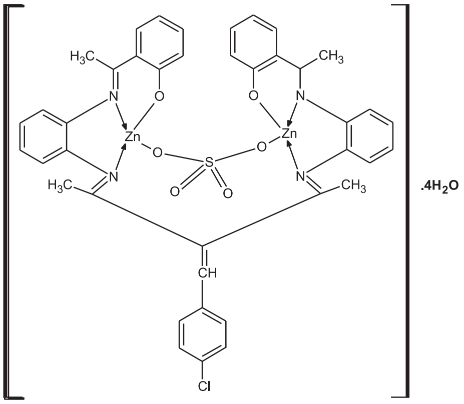
H₃C
CH₃
N
O
O
N
Zn
O
S
O
Zn
O
O
H₃C
N
N
CH₃
.4H₂O
CH
Cl

(9)

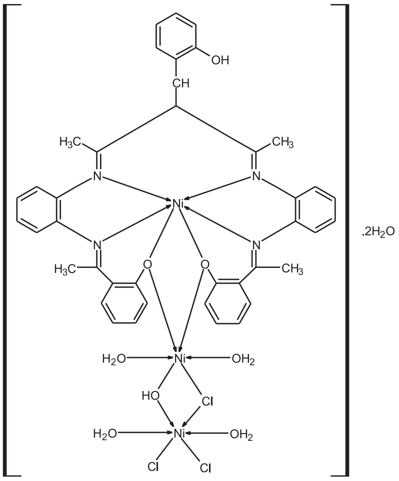
OH
CH
H₃C
CH₃
N
N
Ni
.2H₂O
N
N
H₃C
CH₃
O
O
H₂O
Ni
OH₂
HO
Cl
H₂O
Ni
OH₂
Cl
Cl

(10)

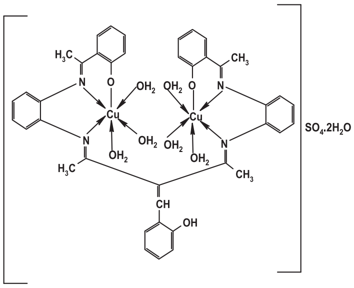

(11)

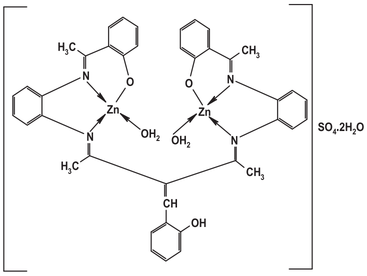

(12)

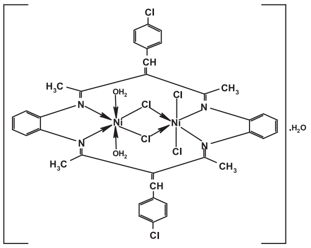

(13)

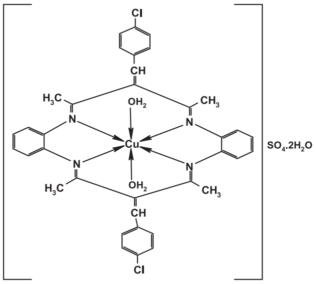

(14)

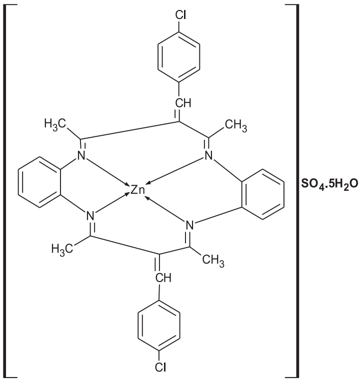

(15)

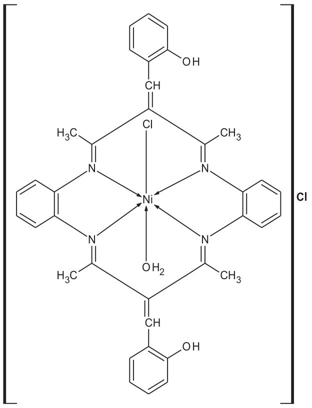

(16)

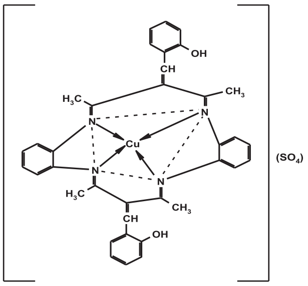

(17)

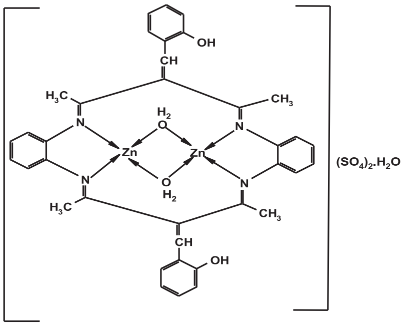

(18)

References

[1] T.W. Hambley, L.F. Lindoy, J.R. Reimers, P. Turner, W. Wei, A.N.W. Cooper, J. Chem. Soc., Dalton Trans. (2001) 614–620.

[2] S. Chandra, L.K. Cupta, Trans. Met. Chem. 30 (2005) 630–635.

[3] T.M.;A. Ismail, J. Coord. 58 (2) (2005) 141–151.

[4] R.R. Fenton, R. Gauci, P.C. Junk, L.F. Lindoy, R.C. Luckay, G.V. Meehan, J.R. Price, P. Tumer, G. Wei, J. Chem. Soc., Dalton Trans. (2002) 2185–2198.

[5] S. Chandra, D. Jain, L.K. Gupta, J. Saudi Chem. Soc. 7 (2003) 243–250.

[6] M.T.H. Tarafder, N. Saravanan, K.A. Course, Trans. Met. Chem. 26 (2001) 613–618.

[7] L. Rousso, N. Friedman, M. Sheves, M. Ottolenghi, Biochemistry 34 (1995) 12059–12065;
T. Bassov, M. Sheves, Biochemistry 25 (1986) 5249–5258.

[8] R.D. Jones, D.A. Summervile, F. Basolo, Chem. Rev. 79 (1979) 139.

[9] R.R. Gagne, C.I. Spiro, T.J. Smith, W.R. Homanh, W.R. Thies, K. Shiemke, J. Am. Chem. Soc. 103 (1981) 4073–4081.

[10] J.E. Kovacic, Spectrochim. Acta 23A (1987) 183–187.

[11] R. Atkins, G. Brfwer, E. Kokto, G.M. Mockler, E. Sinn, Inorg. Chem. 24 (1985) 128–134.

[12] A.D. Garnovskii, A.L. Nivorozhkin, V.I. Minkin, Coord. Chem. Rev. 1 (1993) 126.

[13] L. Canali, D.C. Sherrington, Chem. Soc. Rev. 28 (1999) 85–93.

[14] C.P. Raptopoulou, A.N. Papadopoulos, D.A. Malamatari, E. Ioannidis, G. Moisidis, A. Terzis, D.P. Kessissoglou, Inorg. Chim. Acta 272 (1998) 283–290.

[15] F.H. Fry, B.G. Graham, L. Spicca, D.C.R. Hockles, E.R.T. Tiekink, J. Chem. Soc., Dalton Trans. (1997) 827–833.

[16] M. Rosignoli, P.V. Bernhardt, G.A. Lawrence, M. Maeder, J. Chem. Soc., Dalton Trans. (1997) 323–327.

[17] A. Chaudhary, S. Dave, R. Swarpoop, R.V. Singh, J. Indian Chem. Soc. 79 (2002) 371–377.

[18] X. Xu, Q. Luo, M. Shen, X. Huang, Q. Wu, Polyhedron 16 (1997) 915–919.
[19] A.S. Gaballa, M.S. Asker, A.S. Barakat, S.M. Teleb, Spectrochim. Acta Part A 67 (2007) 114–121.
[20] S. Chandra, L.K. Gupta, Spectrochim. Acta Part A 61 (2005) 269–275.
[21] S. Sarkara, K. Deyb, Spectrochim. Acta Part A 77 (2010) 740–748.
[22] M.M. Omar, G.G. Mohamed, A.A. Ibrahim, Spectrochim. Acta Part A 73 (2009) 358–369.
[23] K. Shankera, R. Rohinia, V. Ravindera, P.M. Reddyb, Y. Hob, Spectrochim. Acta Part A 73 (2009) 205–211.
[24] M.A. Ali, M.H. Kadir, M. Nazimuddin, S.M.M. Majumder, M.T.H. Tarafder, M.A. Khair, Indian J. Chem., Sec. A 27 (1988) 1064–1071.
[25] C.D. Hufford, A.M. Clark, in: Altaur-Rahman (Ed.), Studies in Natural Products Chemistry, Elsevier, Amsterdam, 1988, pp. 421–463.
[26] G. Cross, J.P. Costs, Acad. C.R.S.C. Paris 294 (1982) 173–201.
[27] J.P. Costes, G. Cros, M.H. Darbieu, Y.P. Laurent, Trans. Met. Chem. 7 (1982) 219–228.
[28] D.A. Atwood, Coord. Chem. Rev. 165 (1997) 267.
[29] S. Rayati, N. Torabi, A. Ghaemi, S. Mohebbi, A. Wojtczak, A. Kozakiewicz, Inorg. Chim. Acta 361 (2008) 1239–1245.
[30] F. Marchetti, C. Pettinari, R. Pettinari, A. Cingolani, D. Leonesi, A. Lorenzotti, Polyhedron 18 (1999) 3041–3050.
[31] K. Srinivasan, J.K. Kochi, J. Am. Chem. Soc. 108 (1986) 2309–2320.
[32] E.N. Jacobsen, W. Zhang, A.R. Muci, J.R. Ecker, L. Deng, J. Am. Chem. Soc. 112 (1990) 2801–2803.
[33] E.N. Jacobsen, Acc. Chem. Res. 33 (2000) 421–431.
[34] S. Zolezzi, E. Spodine, A. Decinti, Polyhedron 21 (2002) 55–59.
[35] A.I. Vogel, Practical Organic Chemistry Including Quantitative Organic Analysis, 3rd ed., Longmans, London, 1956, p. 854.
[36] P.W. Selwood, Magnetochemistry, Interscience, New York, 1956, p. 78, 91.
[37] F. Karipcin, B. Dede, S. Percin-Ozkorucuklu, E. Kabalcilar, Dyes and Pigments 84 (2010) 14–18.
[38] W.L. Geary, Coord. Chem. Rev. 7 (1971) 81.
[39] L. Stock, Thermochim. Acta 148 (1989) 149–164.
[40] A.W. Coats, J.P. Redfern, Nature 68 (1964) 201.
[41] C.R. Vinodkumar, M.K. Muraleedharan Nair, P.K. Radhakrishnan, J. Therm. Anal. Cal. 61 (2000) 143–149.
[42] P.B. Maravalli, T.R. Goudar, Inorg. Chem. 17 (1978) 3389–3398.
[43] T.M.A. Ismail, J. Coord. Chem. 59 (3) (2006) 255–270.
[44] K. Nakamoto, Infrared and Raman Spectra of Inorganic and Coordination Compounds, 4th ed., Willey Interscience, New York, 1986, p. 258.
[45] A.A. Saleh, A.M. Tawfik, S.M. Abu-El-Wafa, H.F. Osman, J. Coord. Chem. 57 (4) (2004) 1191–1204.
[46] H. Dietrich, Swiss Patent (1988) 454874.
[47] L.H. Schmidt, Ann. Rev. Microb. 23 (1969) 427–454.
[48] S. Aktiesel, F. Kabet, Dan. Patent (1968) 108625.
[49] D.R. Williams, Chem. Rev. 72 (1972) 203.
[50] K. Nakamoto, Infrared Spectra of Inorganic and Coordination Compounds, 3rd ed., John Willey, 1977.
[51] R. Golbedaghi, S. Salehzadeh, H. Keypour, A.G. Blackman, Polyhedron 29 (2010) 850–856.
[52] A.A. Saleh, J. Coord. Chem. 58 (3) (2005) 255–270.
[53] F.A. Cotton, G. Wilkinson, Advanced Inorganic Chemistry, Interscience Publishers, London, 1974.
[54] S.J. Swamy, S. Pola, Spectrochim. Acta Part A 70 (2008) 929–933.
[55] S. Sreedarana, K.S. Bharathia, A.K. Rahimana, R. Suresha, R. Jegadeeshb, N. Raamanb, V. Narayanana, Spectrochim. Acta Part A 74 (2009) 849–854.
[56] K. Karaoglu, T. Baran, K. Serbest, M. Er, I. Degirmencioglu, J. Mol. Struct. 922 (2009) 39–45.
[57] L. Sacconi, Coord. Chem. Rev. 1 (1966) 126.
[58] F.A. Cotton, G. Wilkinson, Advanced Inorganic Chemistry, 3rd ed., John Willey, 1972.
[59] P.K. Dhara, S. Pramanik, T. Lu, M.G.B. Drew, P. Challopadhyay, Polyhedron 23 (2004) 2457–2464.
[60] M. Sebastian, V. Arun, P.P. Robinson, A.A. Varghese, R. Abraham, E. Suresh, K.K.M. Yusuff, Polyhedron 29 (2010) 3014–3020.
[61] P.F. Rapheal, E. Manoj, M.R.P. Kurup, Polyhedron 26 (2007) 818–828.
[62] M. Mashaly, T.M. Ismail, S.B.E.L. Maraghy, H.A. Habib, J. Coord. Chem. 57 (13) (2004) 1099–1123.